*Published in Goossens, R. (ed.) Remote Sensing in Transition: Proceedings of the 23rd Symposium of the European Association of Remote Sensing Laboratories, Ghent, Belgium, 2-5 June 2003. ISBN 90 5966 007 2, www.millpress.com

Remote Sensing in Transition, Goossens (ed.)

Raw signal simulator for SHARAD

Giovanni Alberti & Giuseppe Salzillo
CO.RI.S.T.A. - Consortium for Research on Advanced Remote Sensing System,Piazzale Tecchio 80, 80125 Napoli, Italy
alberti@unina.it, salzillo@unina.it

ABSTRACT: SHARAD is the new radar sounder sensor for the localization of water under Mars crust that will be flown on the next NASA missions of 2005. The program is funded by the Italian Space Agency (ASI) and, recently, the CO.RI.S.T.A. consortium joined the working group team by participating in sensor performance assessment, simulation and to the definition and realization of the ground equipment (EGSE) employed for the validation of radar.
The present work describes the developed radar signal simulator and shows the preliminary results. The objectives of such a simulator are twofold: the generation of the Mars transfer function to be used within the EGSE and the production of simulated SHARAD raw data to be focused by the ground processing chain.
In both cases, the simulator works in time domain by considering the appropriate superposition of returns from scattering element of the simulated scenario.
The simulator takes into account the satellite trajectory and attitude while the scene is described in terms of height profile and backscattering function of surface and underlying strata. Either isolated scatters and extended targets can be simulated by approximating the scattering surface by square plane facets, large in terms of the incident wavelength but small when compared to the resolution length.
Sub-superficial attenuation and delay are taken into account by considering electromagnetic parameters (permittivity e and conductivity) of the underlying materials.

1 INTRODUCTION

Observations of Mars' surface indicate features similar to those created by ice and water erosion, as rivers, lakes, glaciers, and possibly even an atmosphere was present in the past on Mars.

There is, also, strong evidence that Mars still may contain a significant amount of water within its surface in the form of permafrost, ice, or liquid water. This has driven the attention of the scientific community since the presence of water could provide a better understanding of the geological history of the planet and it could indicate the possibility of past life on Mars. Finally, any accessible reservoirs could provide crucial resources for future manned exploration.

Radar systems will play an important role in the detection of water in any form within the planet's subsurface, and both orbital and lander/rover-based systems (Leuschen, 2001) will need to be used in conjunction to obtain both global coverage along with high-resolution stratigraphy mapping.

In the last few years, NASA and ASI (the Italian Space Agency) were very active in this field and the collaboration has provided the first orbiting sub-sounder instrument, MARSIS (Picardi, 1999) that, defined in the context of the Mars Express mission, will reach Mars at Christmas 2003.

Following this first successful experience and the recommendation of the Mars Reconnaissance Orbiter (MRO) Science Definition Team (SDT), ASI envisaged an instrument whose scientific objectives must be complementary to the MARSIS experiment by exploiting the possibility offered by the Mars Exploration Program (MEP) of 2005.

This has led to the definition of a shallow subsurface sounding radar (SHARAD) (Biccari, 2002) with the primary objective of mapping the distribution of water, both liquid and solid, in the upper portions of the crust of Mars (the penetration depth shall be 300:1000m), at range resolution scales of tens of meters and spatial resolution of the order of some hundred of meters.

The development of the radar has been entrusted to Alenia Spazio and, recently the CO.RI.S.T.A. consortium joined the team by taking part in the definition and implementation of the project requirements of ground test instruments, EGSE (Electrical Ground Support Equipment), and, in particular, to the implementation and validation of MEGS

(Mars Echoes Generation System), which allows to simulate the radar echoes received by Mars surface.

In this framework a radar signal simulator has been developed and in the following its main feature are described and first preliminary results are shown.

2 SHARAD SYSTEM

The radar transmits a chirp signal with center frequency of 20 MHz and with a bandwidth of 10 MHz over a duration of about 300 μsec. The system will also be able to transmit two distinct pulses centered on two slightly different frequencies within the bandwidth of system, respectively 17.5 and 22.5 MHz. In this way, dual frequency measurements are also possible to improve the estimate of the dielectric properties of the subsurface layers and for reduction of the surface clutter which may prevent the subsurface detection.

There are three main subsystems: Antenna, RF and Digital. The antenna will be essentially composed of a dipole radiating element roughly matched in length to half the wavelength of the carrier frequency. An impedance matching network will also be required to match the transmitter and antenna impedances.

The RF sub-system includes the Transmitter, the Tx/Rx switching net and the receiver down to the Analog to Digital Converter.

The Digital sub-system is composed of the Command and Control functions interfacing with the spacecraft bus, the processing capabilities to preelaborate the science data collected during the observations, as well as the digital synthesis of the radar pulse and generation of the system timings.

To reach the 300 – 1000 m spatial resolution requirement, a fully focused synthetic aperture processing is required. A reduced resolution mode could also be envisaged in the radar, with less demanding processing capabilities on board.

2.1 *On ground verification sub-system*

On ground, in order to verify the correct design of the instrument, SHARAD will be subjected to a series of functional electrical, environmental and performance test campaigns. Testing will require a dedicated instrument Electrical Ground Support Equipment representative of the spacecraft to instrument interfaces. EGSE will also include a special sub-system, the MEGS that will acquire actual pulses transmitted by the radar, simulate the Mars response and re-inject into the radar the signal, simulating the echoes that SHARAD would receive from the planet.

Figure 1 shows the MEGS block diagram. The Mars transfer function's FFT (Fast Fourier Transform) is multiplied with the FFT of the transmit signal and a successive IFFT (Inverse FFT) is performed for obtain the received simulated echo.

For each pulse, the Mars transfer function is obtained positioning a discrete impulse at the range bin correspondent to the target-sensor time delay while the impulse amplitude is related to the losses experienced by the signal along its path.

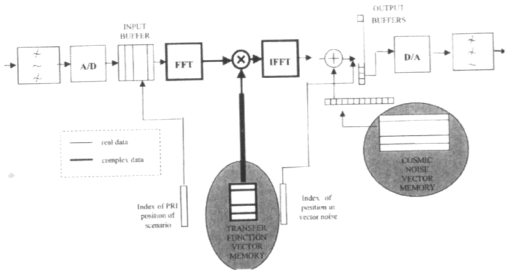

Figure 1. MEGS block diagram

3 SHARAD SIMULATOR

The production of Mars transfer function is one of the results of the developed SHARAD simulator. To this aim, for each satellite position and target of the scene, it is necessary only to evaluate the round-trip time (t_T) and signal amplitude attenuation (A_T) given by spreading losses, antenna gain, target backscattering coefficient and crossed sub-surface strata.

The other possibility is to let the simulator generate SHARAD raw data that means to perform via software what the EGSE does via hardware (the open loop mode of MEGS). In this case the previous two evaluated parameters are used to translate and attenuate a copy of the transmitted signal, such as:

$$x_r(\tau) = A_T \cos\left(2\pi f_0 \tau + \pi\alpha\tau^2\right) \qquad (1)$$

where: $\tau = t - t_D - t_T$

being t_D the radar range gate delay, f_0 is the carrier and α is the chirp rate.

In this way, the signal received by a single target is simulated while the whole set of raw data are given by the superposition in time domain for all the targets forming the scenario.

The functional block diagram of the simulator is shown in Figure 2. The main characteristics of each block are described in the following paragraph.

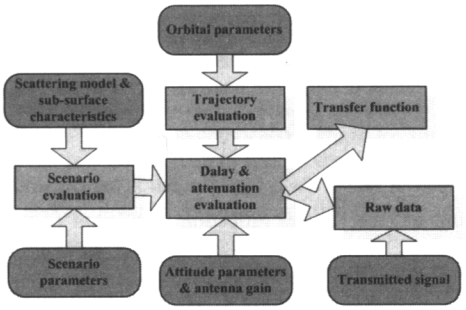

Figure 2. Simulator block diagram

3.1 *Orbital and attitude parameters*

To evaluate the satellite trajectory, the simulator takes into account the actual elliptical orbit around Mars. The orbit position of the satellite is described by its orbital elements:

- a, the semi-major axis of the ellipse;
- e, the eccentricity of the ellipse;
- δ, the inclination of the ellipse;
- β, the true anomaly of the satellite.

The distance between the satellite centre of mass and the Mars' centre is given by the following expression:

$$R_s = \frac{a(1-e^2)}{1+e\cdot\cos(\beta)} \tag{2}$$

which is the equation of an ellipse with semi-major axis a. The maximum and minimum value of R_s are respectively:

$$\begin{aligned} R_{s,\max} &= a(1+e) \\ R_{s,\min} &= a(1-e) \end{aligned} \tag{3}$$

with:

$$a = \frac{(R_{s,\max}+R_{s,\min})}{2} \tag{4}$$

Also the attitude of the satellite is computed, in order to correctly evaluate the antenna gain contribution. This is done by considering a series of reference frames and by passing from one to another by means of appropriate transformation matrices. The frames refer to right-handed Cartesian co-ordinate systems and all rotations are right-handed.

The used reference frames are:

- Central reference frame (IC) (X_{IC}, Y_{IC}, Z_{IC}) that has its origin at the Mars' centre. The fundamental plane is the equator and the positive X_{IC}-axis points toward the ascending node of satellite orbit. The Z_{IC}-axis points in the direction of the north pole and the Y_{IC}-axis is chosen so as to form a right-handed set of co-ordinate axes. This reference frame is shown in Figure 3.
- Orbital reference frame (SC) (X_{SC}, Y_{SC}, Z_{SC}) that has its origin at satellite centre of mass. The orbital plan is the (X_{SC}, Z_{SC}) one. The positive Z_{SC}-axis points toward the Mars' centre and X_{SC}-axis in direction of the satellite velocity vector. The Y_{SC}-axis is chosen so as to form a right-handed set of coordinate axes. This reference frame is shown in Figure 3.
- Body reference frame $(X^0_{BX}, Y^0_{BY}, Z^0_{BZ})$ is fixed in the body of satellite structure with origin at satellite centre of mass. Attitude angles are rotations around appropriate axes: X^0_{BY} for roll, Y^0_{BY} for pitch and Z^0_{BY} for yaw. These angles are positive if measured in counter-clockwise direction and the rotation sequence is assumed to be yaw, pitch and roll.
- Antenna nominal mechanical reference frame $(X^0_{AM}, Y^0_{AM}, Z^0_{AM})$ is fixed to the body reference frame and has origin at satellite centre of mass. The antenna plane is the (X^0_{AM}, Y^0_{AM}) one with the X^0_{AM}-axis directed as the X_{BY}-axis and the Z^0_{AM}-axis normal to this plane and directed as the antenna mechanical boresight.

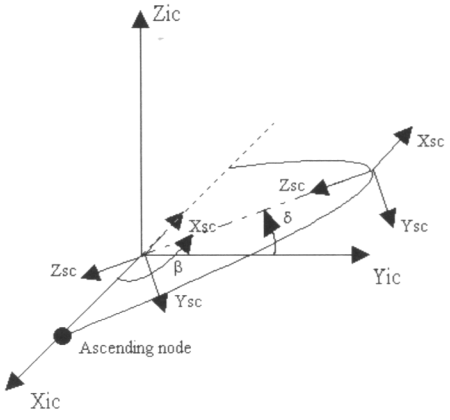

Figure 3. Central and orbital reference frame

3.2 *Scenario definition*

The simulator manages the following scenarios typology:

- isolated mono-dimensional point target scenario;
- isolated bi-dimensional point target scenario;
- bi-dimensional extended scenarios.

In the first two cases the scenario is formed by a certain number of point targets lying on a single line (the satellite sub-track) or on a plane. In this case it is defined an interface limit so the point target can be placed over the surface at a certain altitude and below it at a defined depth.

For the third typology a facet approximation is used. The height profile of the scene is described by an appropriate function, which may be prescribed

either analytically or numerically. This profile is then approximated by square plane facets, large in terms of the incident wavelength but small when compared to the resolution length (the facet number per resolution cell are introduced as input parameter). Each facet is characterized by the co-ordinates of three vertices (or, alternatively, by the co-ordinates of its center and the associate normal) and by a backscattering function. Irregularities of the (macroscopic) terrain profile imply statistical displacements of the facet's vertices, which can be modelled by associating with each facet a random displacement of three of its four vertices with an appropriate probability distribution function (PDF). The extended scene can be either the superficial interface or a sub-superficial one. To evaluate the responses of superficial or sub-superficial interfaces, the electromagnetic field propagation is approximated by ray optics and the refraction at the first interface is taken into account. Of course the simulators considers only surface and sub-surface contribution, while multiple scattering is totally neglected.

3.3 *Surface and sub-surface scattering model*

For the back-scattering coefficient, the classical theory of scattering from a random rough surface can be applied. In particular in Picardi, 2001 it is introduced a fractal geometric description of the surface in the classical Kirchhoff approximation.

This model includes the mostly used geometric optics model (Simpson, 1982):

$$\sigma_0(\theta) = \frac{\Gamma_s^2}{2s^2(\lambda)\cos^4(\theta)} e^{-\frac{tg^2(\theta)}{2s^2(\lambda)}} \tag{5}$$

and Hagfors' model (Hagfor, 1964):

$$\sigma_0(\theta) = \frac{\Gamma_s^2}{8\pi^2 s^4(\lambda)}\left(\cos^4(\theta) + \frac{\sin^2(\theta)}{4\pi^2 s^4(\lambda)}\right)^{-1.5} \tag{6}$$

where θ is the local off-nadir angle, Γ_s^2 is the surface Fresnel reflection coefficient and $s(\lambda)$ is the wavelength-scale r.m.s. slope of the surface.

The Fresnel coefficient depends on the electromagnetic properties of the sub-surface material, i.e. the dielectric constant evaluated at the interface:

$$\Gamma_s^2 = \left|\frac{1-\sqrt{\varepsilon_r}}{1+\sqrt{\varepsilon_r}}\right|^2 \tag{7}$$

The surface r.m.s. slope can be estimated from a previous altimetric mission such as the Mars Orbiter Laser Altimeter (MOLA). Picardi, 1999 estimates a value less than 0.02 rad for large scale and 0.1-0.5 rad for small scale.

By assuming that the sub-surface interface has the same roughness its back-scattered coefficient can be evaluated still by applying the above equations only by replacing the surface Fresnel reflection coefficient with the Fresnel reflectivity for a subsurface layer located at a depth z, such as:

$$\Gamma_{ss}^2 = R_{12}^2\left(1-\Gamma_s^2\right)^2 \int_0^z \alpha(\zeta)d\zeta \tag{8}$$

being R_{12}^2 the Fresnel reflection coefficient of such interface, and α the two-way attenuation per meter due to dielectric dissipation.

Of course, in the above equations the incidence angle θ should take into account the refraction as shown in Figure 4.

All the parameters involved in the previous expression, such as the surface and sub-surface Fresnel coefficients and attenuation, need an electromagnetic characterisation of Martian composition that can be found in literature (Bandfield, 2000). The planet is mainly composed by a basaltic composition in the southern hemisphere and an andesitic composition in the north.

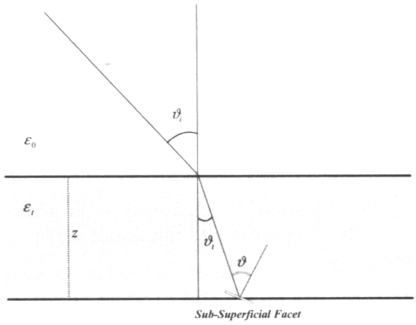

Figure 4. Acquisition geometry

4 SIMULATION RESULTS

An isolated point target scenario can be useful to study the radar impulse response and assess its performance.

SHARAD being an actual nadir-looking SAR (Synthetic Aperture Radar) system, the simulated data should be fully compressed in range and azimuth taking into account range migration and the high percentage bandwidth used. All the images presented in this paper have been processed by using a modified chirp-scaling algorithm (Potsis, 2001).

The parameters used for the simulations are shown in Table 1. These are the actual parameters foreseen for SHARAD but the PRF that will be much higher (about 700 Hz) and a data presumming (32 time) along the azimuth will be performed onboard for reducing the data rate and increasing the achievable SNR (Signal to Noise Ratio). This can

cause some problem of aliasing in the impulse response that can be still analysed by the simulator.

Table 2 shows the characteristics of the isolated target simulations shown in the following, that have been indicated with a capital letter (A, B and C).

Figure 5 shows the compressed image for simulation A while Figure 6 and Figure 7 show the azimuth and range cuts at the response peak. These plots represent the impulse response of the system from which resolution performance can be assessed by means of direct measurement.

If another point target is located just below the previous one at a certain depth (simulation B) an additional weaker spot will appear on the compressed image as shown in Figure 8. The corresponding range cut, shown in Figure 9, allows the measurements of amplitude difference between the two point targets due to sub-surface attenuation and range displacement due to different path and velocity.

In simulation C four point targets are located as to form a rectangle on the surface. Two targets are sub-nadir with respect the radar while the other two are displaced in the across-range direction. The resulting compressed image is shown in Figure 10 while the corresponding range cut is plotted in Figure 11. As expected, the peak of the response of targets in the across-track appear weaker due to the strong decreasing of back-scattering coefficient with the incidence angle. In addition they can be superimposed with returns coming from sub-surface that can be, eventually, totally masked. Therefore the surface acts as clutter by affecting the probability of sub-surface layer detection of the system. This depends on back-scattering model of both surface and sub-surface interfaces and electromagnetic properties of sub-surface and the simulator can give a significant help in understanding the relationships and assessing the detection performance of the radar.

As far as extended scenario is concerned, some preliminary runs have been performed only with surface height profile. In particular a scenario looking like a possible crater on Mars have been generated, as shown in Figure 12. The surface r.m.s. slope has been increased to 0.8 in order allow a broader view of the scenario with the incidence angle.

The compressed image for a first simulation is shown in Figure 13 (left side). In this case, the scenario has a size of about 10x10 Km^2 in across-range and azimuth and its central off-nadir angle is about 5°.

If the central off-nadir angle in set to 0° the size of the scenario should be increased to compensate the increasing of horizontal resolution at nadir. In this case, the resulting compressed image is shown still in Figure 13 for a 50x10 Km^2 in across-range and azimuth scenario.

Table 1. Parameters used for the simulation

PRF [Hz]	50
Transmitted pulse length [μsec]	85
Receiving window length [μsec]	102.4
Transmitted bandwidth [MHz]	15-25
Sampling frequency [MHz]	80
Satellite altitude [Km]	320
Back-scattering model	Hagfors (s=0.06)
Surface Fresnel coefficient [dB]	-9.5
Sub-surface Fresnel coefficient [dB]	-10
Sub-surface attenuation [dB/Km]	0.95

Table 2. Characteristics of isolated point target simulations

Simulation	A	B	C
Scenario typology	1-D	1-D	2-D
Altitude of interface [m]	0	0	0
Target position (range, azimuth, altitude) [Km]	(0, 0, 0)	(0, 0, 0) (0, 0, -0.3)	(0, 0, 0) (10, 0, 0) (0, 0.5, 0) (10, 0.5, 0)

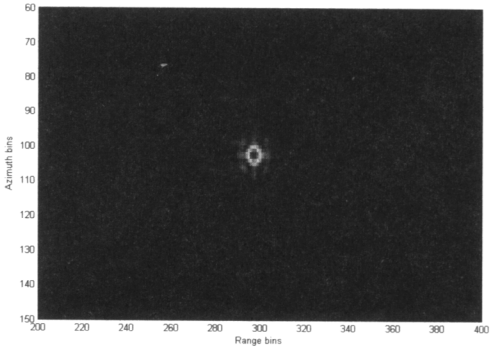

Figure 5. Compressed image for simulation A

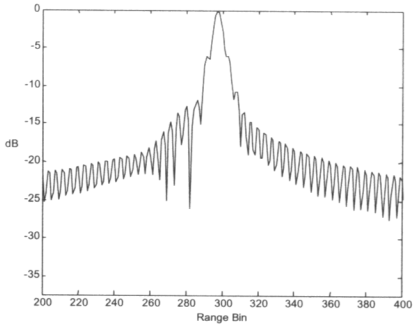

Figure 6. Range line at response peak for simulation A

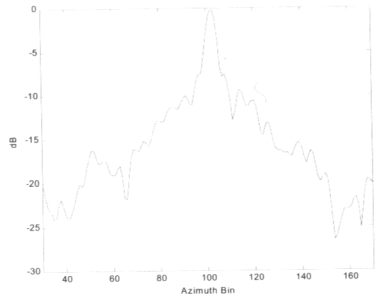

Figure 7. Azimuth line at response peak for simulation A

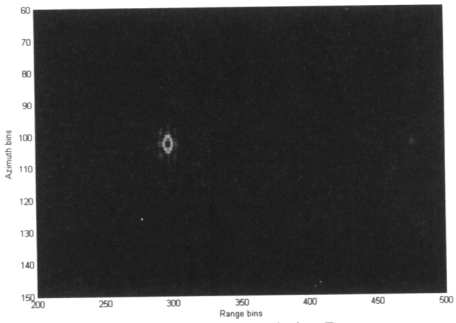

Figure 8. Compressed image for simulation B

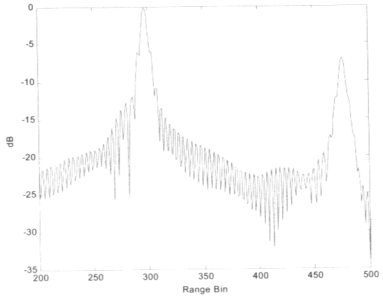

Figure 9. Range line at response peak for simulation B

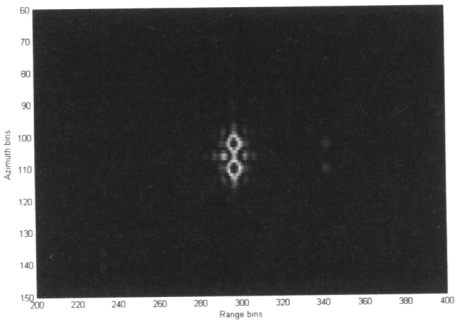

Figure 10. Compressed image for simulation C

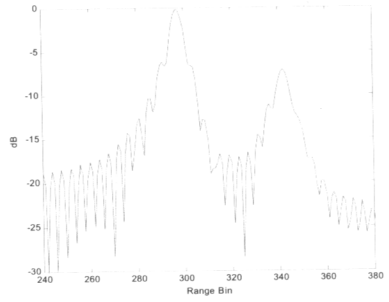

Figure 11. Range line at response peak for simulation C

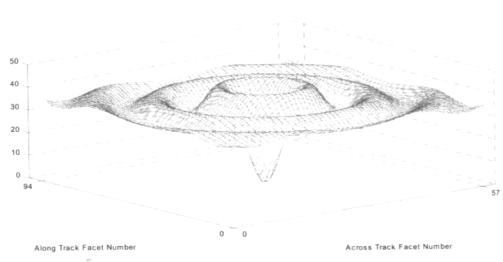

Figure 12. Height profile used for extended scenario simulation

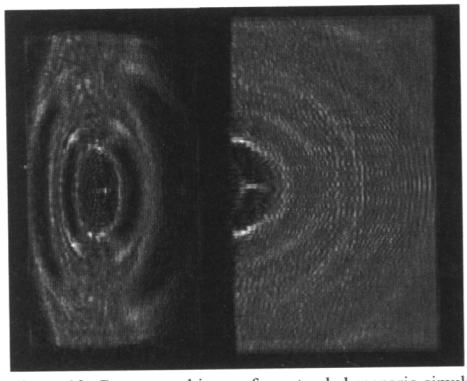

Figure 13. Compressed image for extended scenario simulation (5° of central off-nadir angle on the left and 0° on the rigth)

5 CONCLUSION

A raw data simulator for SHARAD system has been developed and some preliminary results have been shown. This simulator is able to generate the Mars transfer function to be used in the ground validation equipment of SHARAD (MEGS) and to produce raw data to be focused by the ground processing chain.

The simulator works in time domain and takes into account the satellite trajectory and attitude while

the scene is described in terms of height profile and backscattering function of surface and underlying interface. Either isolated scatters and extended targets can be simulated. In the last case a facet approximation is used.

Sub-superficial attenuation and delay are taken into account by considering electromagnetic parameters (permittivity e and conductivity) of the underlying materials.

The software has been coded in MATLAB but a future implementation in ANSI C is foreseen in order to try to speed up executions.

In addition, the possibility of loading actual topographic data derived from other missions (such as MOLA) will be implemented and the database of sub-surface materials will be increased.

ACKNOWLEDGEMENT

This work has been totally funded by the Italian Space Agency (ASI) under the activities of Phase C/D of SHARAD. The authors are also grateful to Enrico Zampolini and Diego Calabrese of Alenia Spazio for the helpful suggestions provided during the development of the program and for those that they will give in the future.

REFERENCES

Bandfield, J.L., Hamilton, V.E., Christensen, P.R. *A global view of Martian surface compositions from MGS-TES*, Science 286, 1626-1630, 2000.

Biccari, D., Picardi, G., Seu, R., *Mars high resolution shallow radar (SHARAD) for the MRO 2005 mission*, Geoscience and Remote Sensing Symposium, 2002. IGARSS '02. 2002 IEEE International, Volume: 4, 2002 Page(s): 2159 -2161

Hagfors, T., *Backscattering from an undulating surface with applications to radar returns from the Moon,* J. Of Geoph. Res. 69,3779-3784, 1964.

Leuschen, C.J., Gogineni, S.P., Clifford, S.M., Raney, R.K., *Simulation and Design of Ground-Penetrating Radar for Mars Exploration,* Geoscience and Remote Sensing Symposium, 2001. IGARSS '01. IEEE 2001 International , Volume: 3 , 2001

Picardi, G., Biccari, D., Seu, R., Orosei, R. *Mars fractal topography applied to Mars Radar for Subsurface and Ionosphere Sounding* (MARSIS), EGS 2001.

Picardi, G., Sorge, S., Seu, R., Plaut, J.J., Johnson, W.T.K., Jordan, R.L., Gurnett, D.A., Orosei, R., Borgarelli, L., Braconi, G., Zelli, C., Zampolini, E., *The Mars Advanced Radar for Subsurface and Ionosphere Sounding (MARSIS): concept and performance*, Geoscience and Remote Sensing Symposium, 1999. IGARSS '99 Proceedings. IEEE 1999 International , Volume: 5 , 1999

Potsis, A., Reigber, A., Mittermayer, J., Moreira, A. and Uzunoglou, N. *Improving the Focusing Properties of SAR Processors for Wide-band and Wide-beam Low Frequency Imaging*, Geoscience and Remote Sensing Symposium, 2001. IGARSS '01.

Simpson, R.A., and Tyler, G.L. "*Radar scattering laws for the lunar surface*", IEEE Trans. Ant. Prop., 30, 438-449, 1982.